Nuclear spin conversion in molecules: Experiments on $^{13}CH_3F$ support a mixing-of-states model

B. Nagels, M. Schuurman, P. L. Chapovsky,[*] and L. J. F. Hermans

Huygens Laboratory, Leiden University, P.O. Box 9504, 2300 RA Leiden, The Netherlands

Using light-induced drift as a tool to separate nuclear spin isomers, we have studied the ortho-para conversion process for gaseous $^{13}CH_3F$ interacting with O_2, N_2, CH_3Cl, and CH_3F itself. It is found that the conversion rate is significantly smaller for collisions with O_2 or N_2 than with CH_3Cl or CH_3F. The data show that intermolecular magnetic interactions do not play a leading role in the conversion. In order to test an alternative model based on mixing of states due to intramolecular interactions, pressure broadening has been measured for these systems. The observed correlation between conversion rates and broadening coefficients supports this mixing-of-states model. [S1050-2947(96)04708-7]

PACS number(s): 34.30.+h, 34.90.+q, 42.50.Vk

I. INTRODUCTION

It is well known that molecules containing two or more identical and equivalent nuclei with nonzero spin occur as different "nuclear spin isomers." A familiar example is ortho- and para-H_2 [1], with total nuclear spin $I = 1$ and 0, respectively. For the total wave function to be antisymmetric under the interchange of two nuclei, as required by Fermi-Dirac statistics for nuclear spin $\frac{1}{2}$, only odd rotational quantum numbers J are allowed for the former and only even J for the latter isomer.

The H_2 case has been the subject of extensive studies over the last three-quarters of a century. Indeed, the interpretation of H_2 spectroscopic and specific heat data in terms of long-lived ortho and para states played a key role in the discovery of the proton spin [2]. More recently, gas-kinetic differences between ortho- and para-H_2 have also been studied, including those pertaining to the nonspherical part of the intermolecular interaction (for a survey see Ref. [3]). Such investigations were made possible by the relative ease of obtaining H_2 in a single isomer form. This is readily achieved by converting normal H_2 (75% ortho) into para-H_2: at low temperature, in the presence of a catalyst like $Fe(OH)_3$, H_2 is rapidly converted to almost 100% para component, the isomer for which $J=0$ is allowed. By contrast, at ambient temperature in the gas phase the conversion is extremely slow: if one avoids interactions with magnetic species like O_2, which create magnetic fields having steep gradients on a molecular scale and break the symmetry, the conversion time is on the order of a year at atmospheric pressure [1].

Conventional wisdom has it that nuclear spin isomers of larger molecules (H_2O, CH_4, NH_3, C_2H_4, CH_3F, etc.) also convert very slowly if no conversion catalyst is used. Indeed, standard quantum mechanics textbooks either ignore the spin conversion or assume that "as with diatomic molecules, owing to the extreme weakness of the interaction between the nuclear spins and the electrons, transitions between states of different nuclear symmetry do not occur in practice" [4]. However, this could never be verified experimentally until recently. The main reason for this was the lack of a practical method to separate the spin isomers. The conversion technique described above for H_2 owes its success to the large rotational level spacing ($B=85$ K) combined with a low boiling point (20.4 K). For heavier molecules temperatures required to achieve a significant change in the spin-isomer abundance ratio are far below the freezing point, and the method fails.

After many unsuccessful attempts to separate the spin isomers of heavier molecules (see, e.g., Ref. [5]) there are now a few methods for separation being applied to I_2 [6], CH_3F [7], H_2CO [8], and H_2O-D_2O [9]. Despite the existence of methods to separate the spin isomers of heavy molecules, virtually nothing is known about their physical properties. There is no experimental work on the influence of the nuclear spin on intramolecular dynamics and chemical reactions (see, e.g., the theoretical treatments of this problem in Refs. [10–12]). Even a fundamental process like the conversion of nuclear spin isomers is actually not studied. This last conclusion is true for all spin isomers studied so far (including H_2), if we are interested in spin conversion in the gaseous phase without catalysts like radicals, magnetic or chemically active particles, etc.

New opportunities in this field have been created by the discovery [13] and the development [14–16] of molecular light-induced drift (LID). This phenomenon combines spectral selectivity with a kinetic mechanism to spatially separate the gas components in a mixture. Since the spin isomers can be spectroscopically distinguished by their spin-specific rotational states—in analogy with H_2—they can be separated by means of LID. Especially important is the fact that with the help of LID, spin isomers can be spatially separated without introducing any additional particles in the system, which may serve as catalysts.

Using this technique it was shown that CH_3F spin conversion can be brought about in the gas phase by collisions with nonmagnetic particles [17]. CH_3F is so far the only known example of spin-isomer conversion in the gas phase. Somewhat surprisingly, it was found that the conversion time for gaseous $^{12}CH_3F$ at 300 K is approximately 1 h at 1 Torr (133 Pa), which is six orders of magnitude shorter than for

---

[*]Permanent address: Institute of Automation and Electrometry, Russian Academy of Sciences, 630090 Novosibirsk, Russia.

H_2. For $^{13}CH_3F$ this was another two orders of magnitude shorter: about 1 min under these conditions. A possible explanation of this unexpected result was suggested [18] on the basis of a mixing-of-states model [19]: It was shown that ortho and para states in a CH_3F molecule can be efficiently mixed by intramolecular magnetic dipole-dipole interactions between molecular nuclei (see Sec. III). Note that the presence of a nuclear spin on the ^{13}C nucleus is not likely to explain the observed difference between $^{13}CH_3F$ and $^{12}CH_3F$, since the F nucleus—at essentially the same distance from the H nuclei—also carries a magnetic moment.

It is the purpose of this paper to supply experimental information yielding insight into the mechanism responsible for the ortho-para conversion process.

II. EXPERIMENTAL APPROACH

We will first briefly outline the essence of LID for gas component separation (for an introductory review on LID the reader is referred to Refs. [15] or [20]). Let us consider a low-pressure gas mixture consisting of a light-absorbing species and an inert buffer gas. The gas is contained in a tube illuminated by a narrow-band tunable laser directed along the tube axis. Let the laser be tuned into the Doppler-broadened absorption profile of an optical transition, i.e., a rovibrational transition. This gives rise to velocity-selective excitation. If, as a result of the excitation, the light-absorbing species changes its kinetic cross section with respect to the buffer gas, the gas will become kinetically anisotropic. This creates a drift of the absorbing species (labeled a) with respect to the buffer gas (b). In a closed tube this produces a concentration difference which is balanced by diffusion in the stationary state.

For the application of LID to the separation of nuclear spin isomers, one of the isomers is the absorbing species (a) while the other serves as a buffer gas (b). Use is made of the fact that the spin isomers can be spectroscopically distinguished since generally—in analogy with H_2—symmetry considerations require that specific nuclear spin states combine with specific rotational states only. The present experiments are performed on the symmetric top molecule CH_3F. The total nuclear spin of the three protons can have the value $I = 3/2$ combining with quantum number $K = 0,3,6,\ldots$ (ortho-CH_3F), or $I = 1/2$ combining with $K = 1,2,4,5,7,\ldots$ (para-CH_3F); here K refers to the projection of the rotational angular momentum upon the molecular axis of symmetry. In equilibrium CH_3F has equal ortho and para abundances (since the larger spin multiplicity of the ortho component is compensated by the smaller number of K values), such that $n_a = n_b$.

A small part of the rovibrational absorption spectrum around 9.6 μm, corresponding to the ν_3 fundamental (C-F stretch), is shown in Fig. 1 for the $^{13}CH_3F$ isotopic species; it illustrates the separate ortho and para absorption lines in the $R(4,K)$ manifold and the tuning range of the $9P(32)$ CO_2 laser line, nearly coincident with the $R(4,3)$ transition in $^{13}CH_3F$.

A scheme of the experimental setup is shown in Fig. 2. Separation of the spin isomers is achieved in a glass tube having an inner diameter of 2 mm and a length of 30 cm. It is filled with $^{13}CH_3F$ at pressures between 0.1 and 2 Torr,
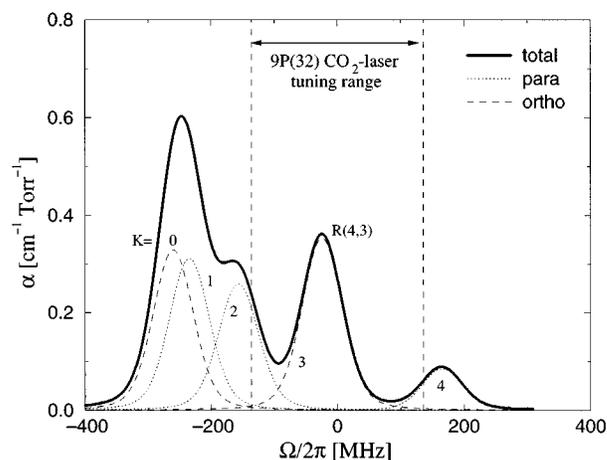
FIG. 1. The rovibrational absorption spectrum of $^{13}CH_3F$ near the $P(32)$ CO_2 laser line in the 9.6 μm band (data from Refs. [21] and [22]). Shown are the $R(4,K)$ transitions, with $K = 0$ through 4. The $R(4,0)$ and $R(4,3)$ transitions pertain to the ortho isomer, the others to the para isomer. The homogeneous linewidth is $\Gamma = 9$ MHz corresponding to $p = 0.5$ Torr (see Table I below).

and illuminated by a frequency tunable waveguide CO_2 laser producing approximately 1 W of radiation in the $P(32)$ line of the 9.6 μm band. The laser is tuned into the blue wing of the $R(4,3)$ absorption line in the ν_3 fundamental vibrational band (cf. Fig. 1), thereby exciting ortho-CH_3F molecules moving away from the laser. For this transition, the collision cross section increases by $\approx 1\%$ [16] upon excitation. As a consequence, due to light-induced drift, ortho-enriched gas will accumulate at the front end of the cell. The rear end is kept at the equilibrium abundance ratio by a large reservoir. The composition at either end is monitored by a differential absorption measurement using two glass probe cells (inner diameter 3 mm, length 11 cm). To this end a power- and frequency-stabilized CO_2 probe laser is used, locked at the
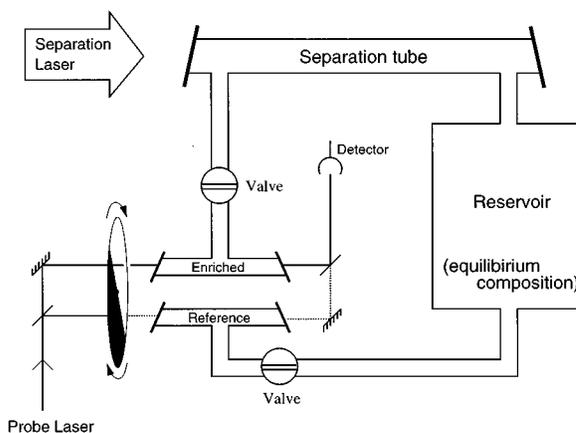
FIG. 2. Schematics of the setup. The separation laser is tuned into the blue Doppler wing of the $R(4,3)$ absorption profile, producing ortho-enriched $^{13}CH_3F$ in the upper probe cell by light-induced drift. After closing the valves the back conversion to the natural abundance ratio is followed by a differential absorption measurement (see Fig. 3 below).
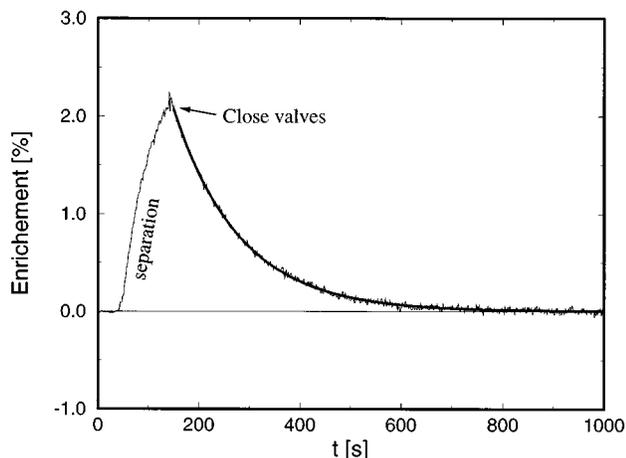
FIG. 3. Typical enrichment decay curve as measured by absorption, for pure $^{13}CH_3F$ at pressure $p=0.6$ Torr. The smooth curve is an exponential computer fit to the data, with the inverse decay time corresponding to the conversion rate γ.

$R(4,3)$ transition frequency of $^{13}CH_3F$. A power of typically 1 mW enters the probe cells. The transmission through the probe cells ("enriched" and "reference," see Fig. 2) is alternately monitored by a single pyroelectric detector, using a chopper at 270 Hz and a lock-in amplifier. The intensities of the two probe beams are set such that zero signal results at zero enrichment. In order to rule out a possible influence of the ν_3 vibration on the conversion, it was verified that the conversion rate was independent of the intensity and thus independent of the fraction of vibrationally excited molecules.

Values for the enrichment $\Delta n_a/n_a$ of the light-absorbing ortho species achieved with 1 W laser power are between 0.5% and 2%, depending on the pressure. After isolating an enriched sample in the upper probe cell (Fig. 2), the time dependence of the differential absorption signal directly reflects the decay of the enrichment. An example is shown in Fig. 3. The conversion rate γ is determined by computer-fitting a function of the form $y=A\,\exp(-\gamma t)+Bt+C$. The constant term in this function accounts for a (usually small) offset due to the change in the $^{13}CH_3F$ to foreign gas ratio during the enrichment stage in the case of mixtures (see Sec. III). Moreover, since the differential detection scheme is very sensitive, some drift in the signal may arise, e.g., due to degassing in one of the detection cells. This was taken into account by the linear term in the fitting function. The exponential term yields the conversion rate γ. It can easily be shown that γ is related to the separate ortho→para and para→ortho transition rates γ_{op} and γ_{po}, respectively, by $\gamma=\gamma_{op}+\gamma_{po}$, where $n_o\gamma_{op}$ is the number of ortho→para transitions per unit time and volume, with n_o the number density of ortho isomers, and similarly for para isomers.

III. RESULTS AND DISCUSSION

Results for γ at different pressures are shown in Fig. 4. The practical pressure range has an upper bound at $p\approx2$ Torr for three reasons. First, the (diffusion-limited) time for enrichment to reach a stationary state increases with pres-
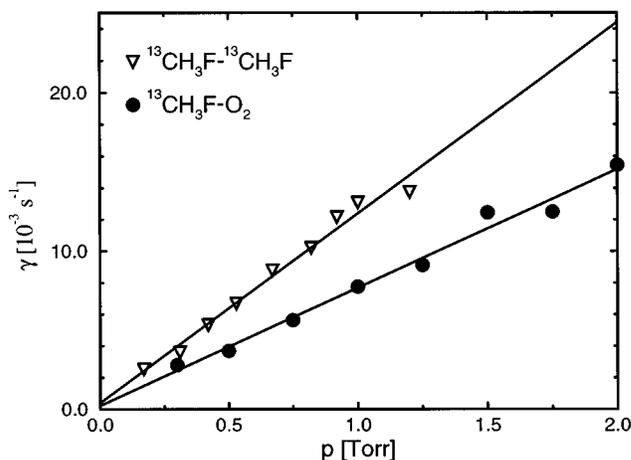
FIG. 4. Results for the conversion rate γ determined from the decay curves (Fig. 3) as a function of total pressure for pure $^{13}CH_3F$ and for a 50:50 mixture with O_2.

sure, while the conversion time decreases. This reduces the achievable separation. Second, pressure broadening limits the velocity selectivity of the LID process, which also reduces separation. Third, pressure broadening reduces the spectroscopic ability to distinguish between the spin isomers (cf. Fig. 1) and thus reduces the detection sensitivity.

For the pressure range studied it is seen from Fig. 4 that γ is linear in pressure, with the slope yielding the gas-phase conversion rate $\gamma/p=12.2\times10^{-3}$ s^{-1} Torr^{-1} for $^{13}CH_3F$, in good agreement with the rate obtained in a completely different setup: $\gamma/p=(14\pm1)\times10^{-3}$ s^{-1} Torr^{-1} [17]. The intercept yields the (small) contribution to the conversion rate from molecule-surface interactions.

In order to study the influence of intermolecular magnetic interactions on the conversion process, the experiments were repeated for an equimolar mixture with O_2, which has a large magnetic moment ($\mu\approx2\mu_B$) in its $^3\Sigma$ ground state. As is well known, in the H_2 case the conversion in the gaseous phase is efficiently catalyzed by O_2. This increase in conversion rate was explained in Ref. [23] on the basis of intermolecular magnetic interactions between H_2 and O_2. The present data show a different behavior for $^{13}CH_3F$. As is seen from Fig. 4 the conversion rate *decreases* significantly when part of the CH_3F molecules is replaced by O_2 (see also [24]). This is seen more clearly from measurements of the conversion rate at fixed total pressure as a function of the O_2 mole fraction $x=n_{O_2}/n$ (see Fig. 5). From extrapolation to $x=1$ it is found that γ_{O_2}, the conversion rate for CH_3F in collisions with O_2, is smaller than the rate in pure $^{13}CH_3F$ by a factor of 4. When comparing this result with the H_2 case one should note that the "fast" H_2 conversion catalyzed by O_2 [1] is still two to three orders of magnitude slower than the conversion of $^{13}CH_3F$ at the same O_2 pressure.

Similar data were taken with N_2 (kinetically rather similar to O_2 except for its magnetic moment, which is three orders of magnitude smaller) and with CH_3Cl (which has a large electric dipole moment, 6.2×10^{-30} C m, equal to that of CH_3F). These results are also displayed in Fig. 5. From the intercepts it is seen that both CH_3Cl and CH_3F are more efficient in producing spin conversion in $^{13}CH_3F$ than O_2,
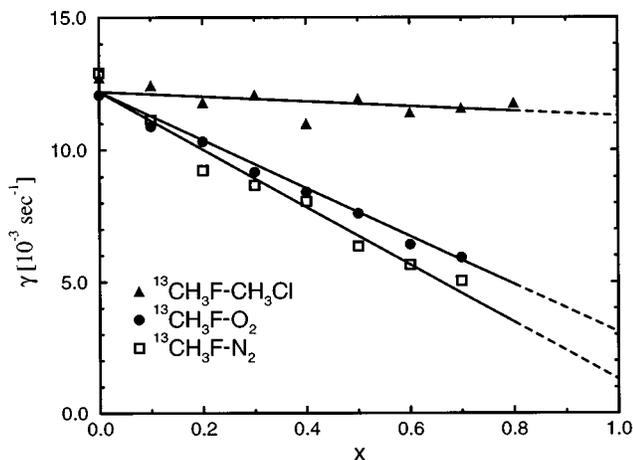
FIG. 5. The $^{13}CH_3F$ conversion rate γ at total pressure $p = 133$ Pa (1.0 Torr) in mixtures with O_2, N_2, and CH_3Cl as a function of mole fraction x of these collision partners. The extrapolated values at $x = 1$ yield the conversion rate of $^{13}CH_3F$ in collisions with O_2, etc.

while N_2 is somewhat less efficient.

It is evident from these data that the magnetic fields produced by the collision partner do not provide the dominant mechanism for the spin conversion in CH_3F.

As an alternative, conversion can be explained [18] by mixing of ortho and para states due to intramolecular interactions (e.g., magnetic dipole-dipole interaction, see below). These interactions can be seen as a small perturbation in the total Hamiltonian. As a consequence of this intramolecular perturbation, the eigenstates of the Hamiltonian are no longer pure ortho and para states, and the total spin of the three protons is not an exact quantum number. The admixture of an ortho component to a para state (and vice versa) will be strongest between ortho and para rotational levels for which the energy gap is small. Due to rotational-level-changing collisions, molecules will continuously move between levels which are weakly mixed (large energy gap) and levels which are strongly mixed (small gap). In this ''mixing-of-states'' model the conversion rate can be expressed in the following general form [18]:

$$\gamma = \sum_{\alpha,\alpha'} \frac{2\Gamma_r}{\Gamma_r^2 + \omega_{\alpha\alpha'}^2} |V_{\alpha\alpha'}|^2 (W_\alpha + W_{\alpha'}). \tag{1}$$

Here Γ_r is the relaxation rate, which can be associated with the rotational level population decay rate, $\hbar\omega_{\alpha\alpha'}$ is the energy gap between ortho (α) and para (α') rotational levels, $V_{\alpha\alpha'}$ is a matrix element of the intramolecular interactions which mix α with α' states, W_α and $W_{\alpha'}$ are the Boltzmann factors of the rotational levels, and the summation has been taken over all ortho and para level pairs.

An issue that lies at the core of this conversion mechanism is the nature of $V_{\alpha\alpha'}$. So far two proposals have been made: magnetic dipole-dipole interaction [18] and spin rotation interaction [19,25]. In the case of magnetic dipole-dipole interactions the ortho and para states are mixed by interactions between F-H, C-H, and H-H-H magnetic moments of the nuclei.

TABLE I. Nuclear spin conversion rate γ for $^{13}CH_3F$ interacting with various collision partners, and homogeneous broadening Γ at 300 K from this work and from Ref. [28].

	γ/p 10^{-3} s^{-1} Torr^{-1}	Γ/p (this work) MHz Torr^{-1}	Γ/p (Ref. [28]) MHz Torr^{-1}
CH_3F-CH_3F	12.2 ± 0.6	18.3 ± 0.6	17.6
CH_3F-O_2	3.1 ± 0.6	4.0 ± 0.5	3.54
CH_3F-N_2	1.3 ± 0.8	5.0 ± 0.5	4.58
CH_3F-CH_3Cl	11.3 ± 0.6	21.7 ± 1.1	

As seen from Eq. (1), at low pressures where $\Gamma_r \ll \omega_{\alpha\alpha'}$ for any ortho-para level pair, the conversion rate is sensitively dependent on $\omega_{\alpha\alpha'}$. Consequently, only the level pairs with small $\omega_{\alpha\alpha'}$ contribute significantly to the conversion, and most of the conversion ''funnels'' through such near-degenerate levels. This model can qualitatively explain the large difference in conversion rate between $^{12}CH_3F$ and $^{13}CH_3F$, observed in Ref. [17], from the differences in the rotational energy level pattern (see Refs. [18,26]).

The present measurements can provide a quantitative check on the plausibility of the mixing-of-states model as the dominant mechanism for the conversion, by using the dependence of γ upon Γ_r [see Eq. (1)]. Since $\Gamma_r \ll \omega_{\alpha\alpha'}$ at 1 Torr [26,27] one should expect approximately $\gamma \propto \Gamma_r$. The quantity Γ_r for CH_3F can now be varied by employing different perturbers.

Using the fact that Γ_r largely determines the spectral-line pressure-broadening coefficient Γ for molecules like CH_3F, we performed measurements of Γ in a separate setup. For these experiments we employed an absorption cell of 2 cm length and 3 mm diameter, and a laser power of ~ 100 μW. First, self-broadening of $^{13}CH_3F$ was determined by measuring the absorption spectrum of the $R(4,3)$ transition at pressures between 0.3 and 1.5 Torr using the full laser tuning range (see Fig. 1). The experimental results were computer fitted to the theoretical pressure-broadened profile, taking all lines of the $R(4,K)$ manifold into account and neglecting any velocity dependence of Γ, i.e., assuming Voigt profiles for the individual lines. The self-broadening coefficient was found from the slope of a Γ vs p plot, yielding the value $\Gamma/p = 18.3$ MHz/Torr. Next, broadening coefficients were determined for CH_3F interacting with O_2, N_2, and CH_3Cl as perturbers (see Table I). To this end the absorption spectrum at a fixed partial CH_3F pressure was measured as a function of perturber pressure p_p, and a similar analysis was applied to obtain Γ. These data are shown in Fig. 6, where the value of Γ at $p_p = 0$ is determined from the self-broadening experiments. The resulting broadening coefficients for O_2 and N_2 compare favorably with literature data from time-domain studies [28], which may be considered to be more accurate (Table I). The value of Γ for CH_3Cl as a perturber is much larger than for O_2 and N_2, and close to the self-broadening by CH_3F. This is expected in view of the long-range dipole-dipole interactions.

If we now use the approximation $\Gamma \approx \Gamma_r$ and neglect the speed and (J,K) dependence of these quantities, we can compare the pressure-broadening results with the conversion
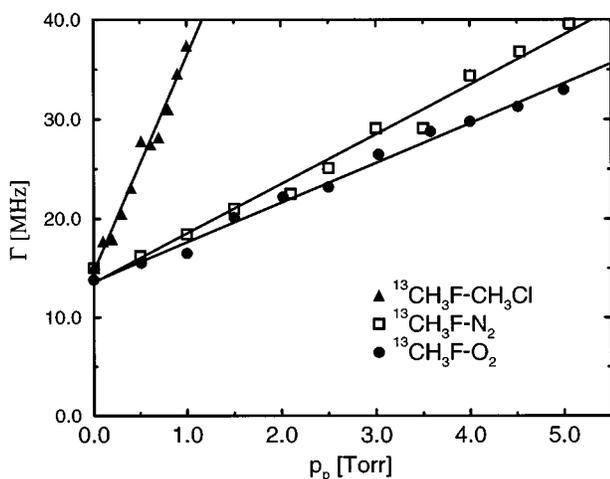
FIG. 6. Homogeneous line broadening Γ as a function of perturber pressure p_p.

data. It is found that the values of the ratio between γ and Γ show qualitative agreement for these gases (Table I). Given the approximations made, one may conclude that the present experiments indicate that mixing of states is the leading mechanism behind nuclear spin conversion in CH_3F. A comparison between O_2 and N_2 suggests that a minor contribution may arise from the interaction between the proton spins in CH_3F and the magnetic field arising from the unpaired electron spins in O_2.

One should note that the magnitude of the ratio γ/Γ is on the order 10^{-9}, i.e., the molecules survive some 10^9 collisions before conversion takes place. This illustrates the smallness of the matrix element $|V_{\alpha\alpha'}|$: using values of $\omega_{\alpha\alpha'}$ for the closest level pair [26] and the corresponding values for W_α and $W_{\alpha'}$ in Eq. (1), one finds $|V_{\alpha\alpha'}|$ to be in the 10^4 Hz range, which is a typical value for nuclear magnetic dipole-dipole interactions.

An additional feature emerging from the conversion experiments is a somewhat surprisingly large influence of supposedly nonmagnetic surfaces. When the gas in the probe cells during conversion was exposed to a small sidearm containing a brass surface of approximately 1 cm^2 the intercepts of the lines in Fig. 4 increased significantly to a value of

4×10^{-3} s^{-1}. In paraffin-coated stainless steel probe cells of the same dimensions, the conversion rate even increased to approximately 9×10^{-2} s^{-1} at $p = 0.5$ Torr. These data show that supposedly nonmagnetic molecule-surface interactions can yield significant conversion efficiencies. This calls for experimental studies to investigate the conversion channels in molecule-solid surface encounters, e.g., by hyperfine Coulomb excitation of metal electron-hole triplet pairs [29,30]. This will be the subject of a separate study.

IV. CONCLUSION

In stark contrast to the H_2 case, the magnetic moment of the collision partner is insignificant for the nuclear spin conversion in CH_3F. This shows that intermolecular magnetic interactions do not provide an important pathway leading to conversion. Instead, a conversion mechanism based on mixing of states due to intramolecular interactions is favored. This is supported by comparing the conversion rate with the observed rotational relaxation rate for different collision partners. Further evidence in favor of the mixing-of-states model may be obtained by studying the conversion at higher pressures. According to Eq. (1) the conversion rate should peak if Γ_r reaches the value $\omega_{\alpha\alpha'}$, for the nearest ortho-para level pair. Since for $^{13}CH_3F$ one has $\omega_{\alpha\alpha'}/2\pi = 130.6$ MHz for the closest (J,K) pair (9,3)-(11,1) [26], and $\Gamma_r = 1.0 \times 10^8$ s^{-1} $Torr^{-1}$ [27], one expects the peak in the conversion rate around 8 Torr. As pointed out in Sec. III, however, experiments at such pressures are not trivial. Alternatively, more detailed information—in particular on the type of intramolecular interaction involved—may be obtained by applying electric fields to shift the energy levels by the linear Stark effect [31]. We hope to clarify the issue in future experiments.

[1] A. Farkas, *Orthohydrogen, Parahydrogen, and Heavy Hydrogen* (Cambridge University Press, Cambridge, England, 1935).

[2] D.M. Dennison, Proc. R. Soc. London Ser. A **115**, 483 (1927); W.F. Giauque and H.L. Johnston, J. Am. Chem. Soc. **50**, 3221 (1928).

[3] F.R.W. McCourt, J.J.M. Beenakker, W.E. Köhler, and I. Kuščer, *Nonequilibrium Phenomena in Polyatomic Gases* (Clarendon Press, Oxford, 1991).

[4] L.D. Landau and E.M. Lifshitz III, *Quantum Mechanics*, 3rd ed. (Pergamon Press, Oxford, 1981), p. 426.

[5] R.F. Curl, Jr., J.V.V. Kasper, K.S. Pitzer, and K. Sathianandan, J. Chem. Phys. **44**, 4636 (1966).

[6] V.I. Balykin, V.S. Letokhov, V.I. Mishin, and V.A. Semchishen, Chem. Phys. **17**, 111 (1976).

[7] L.N. Krasnoperov, V.N. Panfilov, V.P. Strunin, and P.L. Chapovsky, Pis'ma Zh. Éksp. Teor. Fiz. **39**, 122 (1984) [JETP Lett. **39**, 143 (1984)].

[8] J. Kern, H. Schwahn, and B. Schramm, Chem. Phys. Lett. **154**, 292 (1989); B. Schramm (private communication).

[9] V.K. Konyukhov, A.M. Prokhorov, V.I. Tikhonov, and V.N. Faizulaev, Pis'ma Zh. Éksp. Teor. Fiz. **43**, 65 (1986) [JETP Lett. **43**, 85 (1986)]; see also Bull. Lebedev Phys. Inst. No. 1 (1995); No. 5–6 (1995).

[10] M. Quack, Mol. Phys. **34**, 477 (1977).

[11] M. Quack, Stud. Phys. Theor. Chem. **23**, 355 (1983).

[12] M. Quack, J. Chem. Phys. **82**, 3277 (1985).

[13] F.Kh. Gel'mukhanov and A.M. Shalagin, Pis'ma Zh. Éksp. Teor. Fiz. **29**, 773 (1979) [JETP Lett. **29**, 711 (1979)].

[14] G.J. van der Meer, R.W.M. Hoogeveen, L.J.F. Hermans, and P.L. Chapovsky, Phys. Rev. A **39**, 5237 (1989).

[15] L.J.F. Hermans, Int. Rev. Phys. Chem. **11**, 289 (1992).

[16] P.L. Chapovsky, Izv. Akad. Nauk SSSR Ser. Fiz. **53**, 1069 (1989) [Bull. Acad. Sci. USSR, Phys. Ser. **53**, 43 (1989)].

[17] P.L. Chapovsky, Zh. Éksp. Teor. Fiz. **97**, 1585 (1990) [Sov. Phys. JETP **70**, 895 (1990)].

[18] P.L. Chapovsky, Phys. Rev. A **43**, 3624 (1991).

[19] R.F. Curl, Jr., J.V.V. Kasper, and K.S. Pitzer, J. Chem. Phys. **46**, 3220 (1967).

[20] G.J. van der Meer, H.I. Bloemink, E.R. Eliel, and L.J.F. Hermans, J. Mol. Spectrosc. **153**, 419 (1992).

[21] S.M. Freund, G. Duxbury, M. Römheld, J.T. Tiedje, and T. Oka, J. Mol. Spectrosc. **52**, 38 (1974).

[22] S.K. Lee, R.H. Schwendeman, and G. Magerl, J. Mol. Spectrosc. **117**, 416 (1986).

[23] E. Wigner, Z. Phys. Chem. B **23**, 28 (1933).

[24] B. Nagels, M. Schuurman, P.L. Chapovsky, and L.J.F. Hermans, J. Chem. Phys. **103**, 5161 (1995).

[25] K.I. Gus'kov, Zh. Éksp. Teor. Fiz. **107**, 704 (1995) [Sov. Phys. JETP **80**, 400 (1995)].

[26] P.L. Chapovsky, D. Papoušek, and J. Demaison, Chem. Phys. Lett. **209**, 305 (1993).

[27] H. Jetter, E.F. Pearson, C.L. Norris, J.C. McGurk, and W.H. Flygare, J. Chem. Phys. **59**, 1796 (1973).

[28] F. Rohart, H. Mäder, and H.-W. Nicolaisen, J. Chem. Phys. **101**, 6475 (1994).

[29] E. Ilisca, Phys. Rev. Lett. **66**, 667 (1991).

[30] E. Ilisca, Prog. Surf. Sci. **41**, 217 (1992).

[31] B. Nagels, M. Schuurman, L.J.F. Hermans, and P.L. Chapovsky, Chem. Phys. Lett. **242**, 48 (1995).